Hard x-ray Zernike microscopy reaches 30 nm resolution

Yu-Tung Chen,[1] Tsung-Yu Chen,[1] Jaemock Yi,[2] Yong S. Chu,[2,3] Wah-Keat Lee,[2] Cheng-Liang Wang,[1] Ivan M. Kempson,[1] Y. Hwu,[1,4,5,7] Vincent Gajdosik,[6] and G. Margaritondo[6,*]

[1]*Institute of Physics, Academia Sinica, Taipei 115, Taiwan*

[2]*Advanced Photon Source, Argonne National Laboratory, Argonne, Illinois 60439, USA*

[3]*National Synchrotron Light Source II, Brookhaven National Laboratory, Upton, New York 11973, USA*

[4]*Department of Engineering Science and System, National Tsing Hua University, Hsinchu 300, Taiwan*

[5]*Institute of Optoelectronic Sciences, National Taiwan Ocean University, Keelung 202, Taiwan*

[6]*Ecole Polytechnique Fédérale de Lausanne (EPFL), CH-1015 Lausanne, Switzerland*

[7]*e-mail: phhwu@sinica.edu.tw*

**Corresponding author: giorgio.margaritondo@epfl.ch*

Received November 29, 2010; revised February 10, 2011; accepted March 1, 2011;
posted March 11, 2011 (Doc. ID 138601); published March 30, 2011

Since its invention in 1930, Zernike phase contrast has been a pillar in optical microscopy and more recently in x-ray microscopy, in particular for low-absorption-contrast biological specimens. We experimentally demonstrate that hard-x-ray Zernike microscopy now reaches a lateral resolution below 30 nm while strongly enhancing the contrast, thus opening many new research opportunities in biomedicine and materials science. © 2011 Optical Society of America

OCIS codes: 340.0340, 340.7460.

Conventional x-ray microscopy is negatively affected by weak absorption contrast. Zernike solved the corresponding problem in the visible by introducing a quarter-wavelength shift in the relative phase of specimen-scattered and unscattered waves [1]. This enhances the contrast by small phase differences between waves scattered by different specimen areas.

The absorption for hard x rays is typically weaker than for visible light; thus, x-ray microscopy can greatly profit from the Zernike contrast [2–10]. Previous results in the 1990s concerned soft x rays [3,4]. In recent years, 0.3 μm and 60 nm Zernike resolution was achieved for 9 and 4 keV photons [5,6] and then 40–50 nm at 8 keV [7,8].

Recently, absorption microscopy at 8 keV reached a 30 nm resolution [11], a milestone for biomedical imaging of thick specimens. Could Zernike phase contrast reach this milestone? We present here positive evidence: Fig. 1 shows one of the supporting tests. Figures 1(a) and 1(b) are micrographs of a 180 nm thick Au star nanopattern without and with Zernike phase shift. The contrast enhancement of Fig. 1(b) is evident; intensity profiles [e.g., Fig. 1(c)] quantitatively demonstrate a contrast increase by >3.

As to spatial resolution, the power spectrum analysis (PSA) of Fig. 1(d) (discussed below) shows similar resolution in Figs. 1(b) and 1(a): 29 and 31 nm. Thus, the Zernike contrast enhancement is not at the expense of lateral resolution.

These results were obtained with a newly developed x-ray transmission microscope facility (described in [11]) at the Advanced Photon Source (APS), Argonne National Laboratory. Figure 2(a) shows its optical layout; the main components are a capillary condenser to focus the x rays on the sample, a pinhole to eliminate unwanted illumination, a precision sample stage, a Fresnel zone plate (FZP) objective, the detector (a thin CsI scintillator and a CCD plate) and a Zernike phase ring [Fig. 2(b)]. The system is connected to the 32-ID undulator beamline, with a double-bounce Si(111) crystal monochromator.

The facility is equipped with interchangeable objectives acting as phase FZPs, fabricated by the Academia Sinica (Taipei), with a combination of electron-beam writing and electrodeposition [11]. The outer zone width is either 30 or 45 nm, and the absorber is 450 or 700 nm thick Au; different FZP diameters provide optimal focusing for 8–12 keV photon energies. The space frequency bandwidth reaches 35 μm^{-1}. Depending on the Au thickness, the FZP efficiency is 1% or 3%, <5% of the theoretical values, a loss attributed to slight pattern imperfections and reduced Au density yielded by electrodeposition. The detector pixel resolution is 5 nm.

The Zernike phase ring, located [Fig. 2(b)] at the condenser conjugate plane (near the back focal plane of the objective zone plate), is made of electroplated Au on a

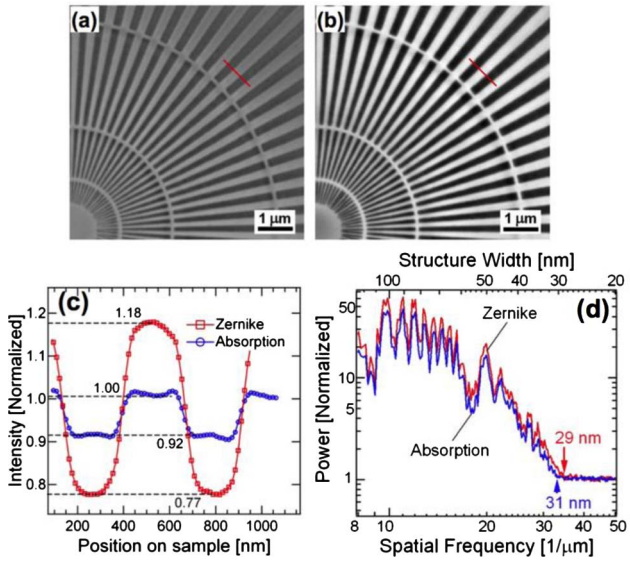

Fig. 1. (Color online) (a), (b) Micrographs of a 180 nm thick Au star test pattern obtained with absorption and Zernike phase contrast. (c) Intensity profiles along the red lines in (a) and (b). (d) Power spectra assessing the spatial resolution.

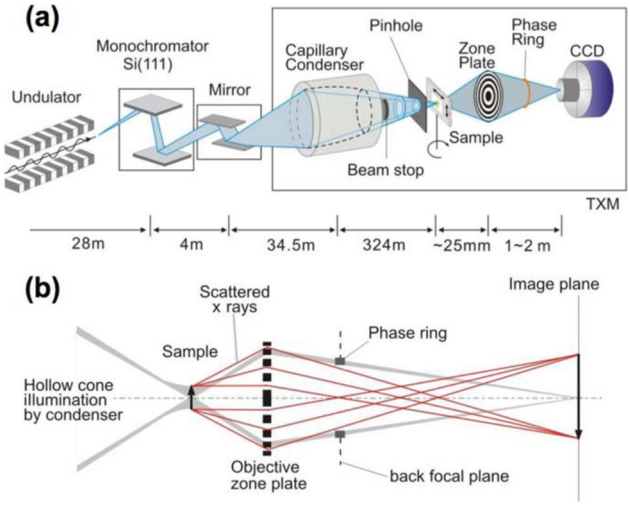

Fig. 2. (Color online) (a) Layout of the transmission x-ray microscope (TXM). (b) Geometry for the Zernike phase contrast.

silicon nitride membrane. Its thickness is selected to phase shift the incident radiation beam by $3\pi/2$ for the following reason. For weak scattering, the phase transmittance function is $\exp(i\Omega) \approx 1 + i\Omega$ and its magnitude is 1. A $3\pi/2$ phase shift of the incident beam changes the phase factor to $\approx -i + i\Omega$, magnitude $\approx 1 - 2\Omega$, making the object image darker and more visible. This is better than a $\pi/2$ shift that would give a phase factor $\approx i + i\Omega$, magnitude $\approx 1 + 2\Omega$ and a brighter object image. In fact, except for a pure phase object, x-ray absorption is also present and works against the effects of the $\pi/2$ shift but enhances those of the $3\pi/2$ shift.

Alignment is critical: a "Bertrand lens" [12] (a limited-resolution FZP) is used to position the phase ring with respect to the unscattered annular illumination of the sample. This lens images at the detector the illumination at the condenser conjugate plane. All condensers are optimized for phase contrast. This means that the annular illumination is narrow: the illuminated area is $\approx 10\%$ of the FZP area; thus most of the scattered x rays are unaffected by the phase ring and can produce phase contrast.

Our key objective, lateral resolution, required a careful analysis of aberrations and artifacts. To assess thickness-related effects, we tested at 8 keV three rings with thickness of 2.5, 2.6 (optimal), and 2.7 μm, and the same width and diameter, 4.5 and 68 μm. The 2.5 and 2.7 μm rings produced very limited contrast in images like Fig. 1, while causing circular blurring and strong differential contrast in the outer image region due to phase aberrations.

We assessed these effects by PSA of the images after pixel-by-pixel multiplication by a Hanning window function to avoid edge effects. The two-dimensional Fourier transformation of the image was squared and azimuthally integrated over 2π. The resulting PSA curves show that frequency cutoff is worse for the nonoptimal thicknesses. PSA also revealed aberrations effects caused by the ring diameter. On the other hand, we could improve the resolution by fine tuning the photon energy in 50 eV steps: the optimum value was 7.95 keV.

Figure 3 shows results for nearly phase objects, polystyrene particles [$(C_8H_8)_n$], at 8 keV, where the refractive

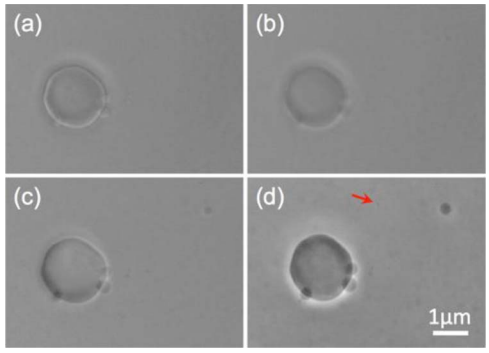

Fig. 3. (Color online) Image of polystyrene particles: (a)–(c) absorption images, (b) in focus and (a), (c) 20 μm before or after focus. (d) Zernike phase contrast image with a 100 nm particle marked by the arrow.

index is $n = 1 - \delta - i\beta$ with $\delta = 3.88 \times 10^{-6}$ and $\beta = 5.58 \times 10^{-9}$. The absorption images, Figs. 3(a)–3(c), in focus or slightly out of focus, only show edge-enhanced contrast, whereas the Zernike image [Fig. 3(d)] reveals contrast enhancement by a factor ≈2.

Figure 4 shows the importance of <30 nm resolution for biology specimens. An absorption image of an EMT (transplantable murine mammary carcinoma) cell is shown together with two phase contrast images obtained with Zernike rings with the same thickness and diameter and different widths. The width-optimized ring (4.5 μm) gives the best image, Fig. 4(c), whereas the others are more blurred. PSA [Fig. 4(d)] corroborates this conclusion. Such effects are even stronger in Fig. 5, showing an EMT cell cocultured with Au nanoparticles.

The Zernike ring can eliminate other problems affecting absorption images, such as spherical aberration [13] and the noise related to the synchrotron light coherence [14]. Note, however, that x-ray Zernike phase contrast is not beneficial for all samples. For thick (several

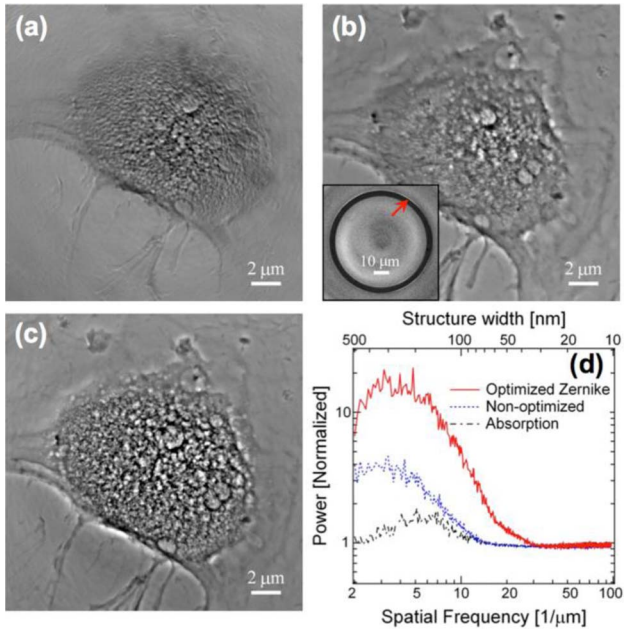

Fig. 4. (Color online) Images of an EMT cell by (a) absorption and Zernike contrast by (c) an optimized ring or (b) a slightly narrower ring (the inset shows the illumination leaking). (d) PSA confirms that the optimized ring yields the best results.

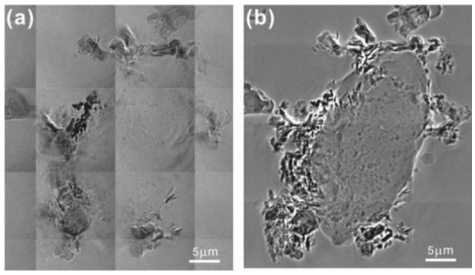

Fig. 5. Images of an EMT cell cocultured with Au nanoparticles, taken (a) without or (b) with a Zernike ring.

micrometers) specimens, it can decrease the contrast with respect to absorption because of phase shifts from areas slightly below or above the focused plane. For wide specimens, it can reduce the contrast for the object center due to the "shading off" effect [15]. It can also produce halo effects affecting the sample morphology analysis.

These issues notwithstanding, a 30 nm resolution is a remarkable progress for hard x-ray microscopy (for reference see, e.g., [9] and [10]), and Zernike contrast at this resolution opens opportunities not only in biology, medicine, and bioengineering but also in materials science and other areas.

Research was supported by National Science and Technology for Nanoscience and Nanotechnology, the Thematic Project of Academia Sinica (Taiwan), the Fonds National Suisse, and the Center for Biomedical Imaging (CIBM). We used equipment of the Academia Sinica Core Facility for Nanoscience and Nanotechnology and Biomedical NanoImaging. The APS is supported by the United States Department of Energy (DOE) under contract DE-AC02-06CH11357.

References

1. F. Zernike, Science **121**, 345 (1955).
2. D. Rudolph and G. Schmahl, B. Niemann, in *Modern Microscopies, Techniques and Applications*, A. Michette and P. Duke, eds. (Plenum, 1990), p. 59–67.
3. G. Schmahl, D. Rudolph, P. Guttmann, G. Schneider, J. Thieme, and B. Niemann, Rev. Sci. Instrum. **66**, 1282 (1995).
4. G. Schneider, Ultramicroscopy **75**, 85 (1998).
5. U. Neuhäusler, G. Schneider, W. Ludwig, M. A. Meyer, E. Zschech, and D. Hambach, J. Phys. D **36**, A79 (2003).
6. H. Yokosuka, N. Watanabe, T. Ohigashi, Y. Yoshida, S. Maeda, S. Aoki, Y. Suzuki, A. Takeuchi, and H. Takano, J. Synchrotron Radiat. **9**, 179 (2002).
7. A. Tkachuk, F. Duewer, H. Cui, M. Feser, S. Wang, and W. Yun, Z. Kristallogr. **222**, 650 (2007).
8. Y. S. Chu, J. M. Yi, F. De Carlo, Q. Shen, W.-K. Lee, H. J. Wu, C. L. Wang, J. Y. Wang, C. J. Liu, C. H. Wang, S. R. Wu, C. C. Chien, Y. Hwu, A. Tkachuk, W. Yun, M. Feser, K. S. Liang, C. S. Yang, J. H. Je, and G. Margaritondo, Appl. Phys. Lett. **92**, 103119 (2008).
9. M. Stampanoni, R. Mokso, F. Marone, J. Vila-Comamala, S. Gorelik, P. Trtik, K. Jefimovs, and C. David, Phys. Rev. B **81**, 14105 (2010).
10. H. S. Youn and S.-W. Jung, J. Microsc. **223**, 53 (2006).
11. Y.-T. Chen, T.-N. Lo, Y. S. Chu, J. Yi, C.-J. Liu, J.-Y. Wang, C.-L. Wang, C.-W. Chiu, T.-E. Hua, Y. Hwu, Q. Shen, G.-C. Yin, K. S. Liang, H.-M. Lin, J. H. Je, and G. Margaritondo, Nanotechnology **19**, 395302 (2008).
12. D. B. Murphy, *Fundamentals of Light Microscopy and Electronic Imaging* (Wiley, 2001).
13. A. G. Michette, *Optical Systems for Soft X-rays* (Plenum Press, 1986).
14. D. L. White, O. R. Wood, II, J. E. Bjorkholm, S. Spector, A. A. MacDowell, and B. LaFontaine, Rev. Sci. Instrum. **66**, 1930 (1995).
15. A. H. Bennet, H. Jupnik, H. Osterberder, and O. W. Richards, *Phase Microscopy* (Wiley, 1951).